CONTENTS — G through L

CHARACTERIZING AND NAVIGATING SMALL BODIES WITH IMAGING DATA. R. W. Gaskell[1], O. Barnouin-Jha[2], D. Scheeres[3], T. Mukai[4], S. Abe[4], J. Saito[5], M. Ishiguro[5], T. Kubota[5], T. Hashimoto[5], J. Kawaguchi[5], M. Yoshikawa[5], K. Shirakawa[6], T. Kominato[6], N. Hirata[7], H. Demura[7]. [1] Planetray Science Institute. PO Box 135, Altadena, CA 91003, rgaskell@psi.edu , [2]APL/JHU, [3]U. Michigan, [4]Kobe University, [5]JAXA/ISAS, [6]NEC Aerospace Systems, [7]U. Aizu

Introduction: Missions such as Deep Interior [1], which would have mapped the interior of a small asteroid with radar tomography, require a detailed knowledge of both shape and surface topography of the body as well as accurate determinations of the spacecraft position. Recent applications of stereophotoclimometry and navigation estimation to small bodies have proven to be more than adequate for satisfying the requirements of such missions. During the recent Hayabusa mission to Itokawa, about 600 AMICA science images were analyzed. The asteroid's shape and topography were characzterized to about 20 cm, and the spacecraft's position was found to a few meters at the home position range of 7 km. For such small bodies, an additional data type such as laser or radar ranging must be used to set the global scale.

Itokawa: On 12 September 2005, the Japanese Hayabusa spacecraft arrived at the asteroid 25143 Itokawa. Due to Itokawa's small size (500 meters) and low gravity, the spacecraft did not orbit, but hovered near each of two stations on a line between the asteroid and Earth. It remained at the "Gate Position" at a range of about 18 km until September 30, and then shifted to the "Home Position" at a range of about 7 km. Between October 8 and 28, it made several excursions to higher phase locations to obtain varying illumination conditions, and away from the equator to obtain polar data. On November 4, 9 and 12, the spacecraft made approaches to the asteroid in preparation for touchdowns on November 20 and 26.

A set of about 800 landmark maps (L-maps) was constructed from the science images using stereophotoclinometry [2]. These maps were used to construct a global topography model (GTM), to estimate the pole, and to determine the spacecraft's location. Since this was not an orbital mission, LIDAR was needed to set the range, and with that extra data type the spacecraft position was found to about 1.5 meters near the home position. The pole determination had an uncertainty of about .005 degrees, and the landmark locations had rms residuals of about 20 centimeters. The L-maps play the role of body-fixed control points, which can be correlated with imaging data under any illumination or geometry. Their correlation with wide-angle navigation images from the November 12 approach determined the spacecraft trajectory and enabled a solution for Itokawa's mass..

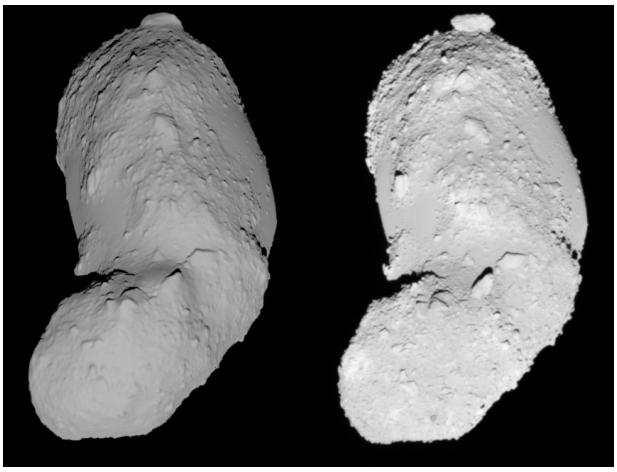

Figure 1. Illuminated Itokawa GTM and corresponding AMICA image.

Eros: In an ongoing study using the NEAR imagina data, the asteroid Eros has been tiled with over 6000 L-maps of varying resolution. Surface residuals are less than 3 meters. With the spacecraft positions assumed to be correct, the camera pointing residuals are less than 20 μrad from L-map correlation, less than a sixth of the best previous value. Work is now underway to incorporate NEAR laser altimeter ranges as a data type to improve the spacecraft ephemeris.

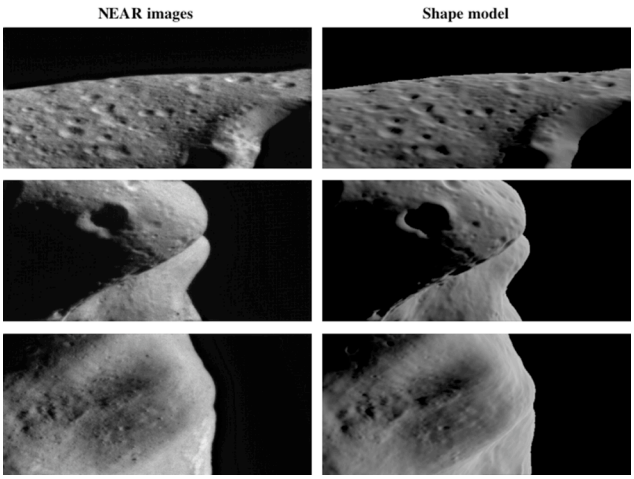

Figure 2. NEAR images and illuminated Eros GTM.

The Gravity harmonics predicted from a homogeneous GTM are much closer to the observed values

than those of previous models, indicating a more uniform interior mass distribution [3]. It is believed that the remaining residuals are due to noise in the determination of the gravity harmonics which may be reduced by the improved knowledge of the spacecraft positions.

Navigation Strategies: For missions to very small bodies, orbiting is not an option due to solar pressure, so that the scale cannot be set by a combination of dynamics and Doppler. Some sort of ranging device, either laser or radar, is essential. Initially, tha body-relative spacecraft locations are found through a combination of accurate camera pointing and range to the as yet undetermined surface. With these data and the ensemble of images, a fairly accurate shape and topography model can be constructed. The largest errors in the model are global ones due to the overall scale.

At this stage of the Itokawa analysis, there was a 0.5% difference between ranges determined by the LIDAR and the ranges predicted from the GTM and the spacecraft ephemeris. This amounted to about 35 meters at the 7 km home position and a 1 meter error in the GTM. Once corrections were made in the ephemeris, a single iteration, the range errors were at the meter level and the ephemeris-related GTM errors were negligible.

The 20 μrad errors quoted above for Eros tell us how well the footprint of the camera on the surface is known. There can be larger pointing errors which are offset by cross- or down-track spacecraft position errors. In order to minimize these errors for the Hayabusa data, a free fall trajectory was fit to the position data between maneuvers. This averaged down the ephemeris errors to the 1.5 meters quoted above, and simultaneously reduced the pointing errors.

It is probable that the same level of accuracy can be achieved with radar ranging, assuming that the return from a precisely determined topography can be adequately modeled. This would provide about quarter wavelength position uncertainties for a 50 Mhz ground penetrating radar.

References: [1] Asphaug, E., et, al, Exploring Asteroid Interiors: the Deep Interior Concept , LPS XXXIV Abstract #1906. [2] Gaskell, R.W., J. Saito, M. Ishiguro, T. Kubota, T. Hashimoto, N. Hirata, S. Abe, O. Barnouin-Jha, and D. Scheeres, Global Topography of Asteroid 25143 Itokawa, LPS XXXVII Abstract 1876. [3] Gaskell, R., A. Konopliv, O. Barnouin-Jha, and D. Scheeres, High Resolution Global Topography of Eros from NEAR Imaging and LIDAR Data, AGU Spring Meeting, Baltimore, May 2006

COMET AND ASTEROID SEISMOLOGY. P. E. Geissler, U.S. Geological Survey, Astrogeology Program, 2255 N. Gemini Dr., Flagstaff, AZ 86001 USA; pgeissler@usgs.gov.

A fundamental question about near Earth objects is the nature of their interior structure. No geophysical technique addresses this question better than seismology, from which most of our knowledge of the interior structure of the Earth is derived. Seismology provides information about the mechanical properties of geologic materials, that in turn constrains their physical state. Measurements of the velocity of seismic signals yield the elastic moduli along the ray path, if the density is known. Measurements of body wave amplitude and attenuation as a function of distance provide information on the anelastic response of the object, related to the packing, cohesion and coupling between particles. Mechanical discontinuities in the interior of the asteroid will produce scattering of the seismic signals, resulting in an extended envelope of acoustic noise after the first arrivals of the body waves. Observations of the period and decay of whole-body oscillations constrain the homogeneity, interior structure and bulk anelastic response of the target.

The most basic parameter to be measured on a small body is the speed of sound through the object. The compressional (P wave) sound speed in natural materials varies from a few hundred meters per second in dry, unconsolidated alluvium up to 3,000 to 5,000 m/s in competent ice or rock. Thus a simple measurement of the travel time of the first arrival of a seismic signal traversing an asteroid would be sufficient to distinguish a gravitationally bound rubble-pile from a monolithic rock fragment. A comprehensive experiment that maximizes the information acquired would involve multiple sources and detectors that employ 3 axis detectors with a broad range of frequencies and sensitivities. The need for multiplicity stems from our desire to measure signal attenuation, particularly with unknown coupling between the source and target, which also drives the requirement for detectors with a wide dynamic range of sensitivity. Three axis detectors are needed to distinguish shear (S wave) displacements. The range of frequencies to be covered ranges from ~1 Hz for whole-body oscillations up to several hundred Hz for late arriving acoustic noise.

The main challenge for sounding small bodies is the risk that the detectors could be lofted off of the surface, should the peak seismic acceleration exceed the weak gravity of the target body. Calculations show that for bodies larger than ~1 km in diameter, there is comfortable overlap between their gravitational acceleration and the seismic accelerations that can be detected using established technology. For smaller bodies, the risk can be mitigated by using a variety of source energies and employing sensitive (but fragile) detectors sensitive to accelerations as small as 10^{-7} g. In any case, the travel times and amplitudes of P wave first arrivals will be obtained even if the detectors are subsequently shaken from the surface of tiny targets.

A simple strategy for sounding the interior of a small body would be to place two sets of seismic stations consisting of identical sources/receivers on opposite sides of the object and detonate them sequentially. When the first station is detonated, the neighboring station of the pair will monitor the strength of the blast in the near field while the stations on the opposite side of the target will record the arrival times and amplitudes of the signals traversing the interior and the surface of the asteroid. In this way, the source accelerations can be measured accurately even though the coupling of the explosive energy to ground motion can not be predicted in advance. This procedure will yield both the velocity and attenuation of sound waves inside the object, sufficient to determine the interior structure of the asteroid. The experiment could be performed with only 3 stations, but the fourth provides redundancy and ensures that the complete set of science measurements can be obtained if any one of the stations were to fail. The second station to be detonated will be one of the pair on the opposite side of the object, repeating the full set of science measurements. The two remaining stations could still complete the primary measurement objective of determining the speed of sound through the interior of the object. The detonation of the final station could only be viewed from orbit but would still add to our knowledge of the object's surface properties and of the dynamics of cratering. Each station would be equipped with 2 sets of three-axis piezo-electric accelerometers with different sensitivities. The primary detectors are robust, low-sensitivity accelerometers with extensive flight heritage that are unlikely to saturate during the impact of the instrument onto the surface and will accomplish the primary objective of measuring the velocity of body waves traversing the asteroid. The secondary accelerometers are far more sensitive, enabling studies of tidal flexure and the damping of whole-body oscillations, but are more fragile and thus riskier than the primary detectors. The dual systems provide redundancy in achieving the chief science objectives and resiliency in case of in-

strument failure. They also provide some insurance for circumstances where source strength and target attenuation are poorly known, by extending the dynamic range of the seismic signals that can be recorded.

In summary, active seismic experiments afford an effective means to explore the interior structure of small celestial bodies. They probe the mechanical properties of the interior, complementing studies of electromagnetic and other properties. Seismic experiments can be inexpensive, made up of simple explosives and arrays of accelerometers that are available off the shelf at low cost. They can be combined with more ambitious studies of the surface, including dynamic processes such as cratering, ejecta dynamics, and seismic shaking. With a history of terrestrial, lunar, and Martian applications, seismology will add solid science to future NEO missions with very little perceived risk.

A REVIEW OF PENETROMETERS FOR SUBSURFACE ACCESS ON SMALL SOLAR SYSTEM BODIES. D. Glaser,[1]P. Bartlett[2], K. Zacny[1], S. Gorevan[2,] [1]Honeybee Robotics, P.O. Box 370, Moffett Field, CA, 94035 USA, [2] Honeybee Robotics, 60 W. 34th St., New York, NY, 10001.

Introduction: For the purposes of planetary exploration, penetrators can loosely be defined as sharply pointed structures that are inserted into the soil/regolith with a purely axial force (as opposed to drills, which primarily use a rotating, lateral force). If some aspect of the penetration behavior is used to determine the mechanical properties of the soil/regolith, then the device can also be considered to be a penetrometer. For the study of asteroid and comet subsurfaces that are made of granular materials, penetrators could be used to deploy seismic, thermal, or chemical analysis hardware to depths of perhaps 1-3 m. If used as a penetrometer, the penetrator would be integrated with accelerometers, force gages, and/or depth sensors that would indirectly measure the soil resistance or skin friction. This paper reviews a variety of penetrometer architectures, some of which have already been developed for planetary exploration. From the perspective of comet and asteroid study, one of the principal design factors is the very low gravity, which will have major implications on the interaction between a penetrator and the soil, as well as on the mechanical means of penetrator deployment.

Cone Penetrometers: Civil engineers often use cone penetrometers, long cylindrical rods with a standardized, pointed cone at one end, to measure soil strength. The maximum depth to which such a penetrometer can travel is a function of the length of the rod (which loosely translates into mass for a space mission) and the increase in frictional force as the penetrometer gets deeper.

Static Cone Penetrometer (SCP). As the name implies, the SCP is pushed into the soil with a static force. In terrestrial applications, the static force generally must be on the order of hundreds or thousands of Newtons, which would be unobtainable from a small lander in the low gravity of an asteroid or comet. However, in the case of a small body, where the overburden pressure is much lower than on Earth [1], the amount of force required may be significantly lower. An innovative source of force for a planetary SCP is the kinetic energy of a soft landing spacecraft. A small penetrometer of this type was successfully used on the Huygens probe for its landing on Titan in 2005.

Vibrating Static Penetrometer. In the construction industry, vibration is sometimes used to insert piles into loose soils. The vibration causes a temporary liquefaction of the soil that effectively reduces the amount of axial force necessary to push the pile into the soil. The vibration is generally produced by two counter-rotating eccentric masses, but other methods are also possible. This method of penetration is currently being considered for use on the Moon [2].

Dynamic Cone Penetrometer (DCP). The DCP penetrates by virtue of high energy impacts from a sliding hammer that is dropped onto the penetrating rod. It does not require a reaction force for penetration to occur. In low gravity, however, dropping the hammer onto the rod would not supply enough kinetic energy, so the hammer mass would require some type of downward accelerating mechanism. There are many possible ways of doing this and, in a previous project for the Army Corp of Engineers, Honeybee Robotics developed a number of concepts for a mechanized DCP [3].

Percussive Cone Penetrometer. A variation of the mechanized DCP is to hammer the rod into the subsurface with a small mass that impacts at high velocity and high frequency. This is identical to the mechanism used in hammer drills, minus the rotation of the drill. Honeybee Robotics has performed experiments with a commercially available percussive mechanism that uses a 100 g mass, impacting with 3.4 J of kinetic energy, at a rate of 34 Hz. This system easily penetrated to a depth of 1 m in moderately strong soils [3].

Mechanical "Mole". A mole is a self-propelling cone penetrometer with an internal hammering mechanism consisting of a hammer mass that is accelerated, usually by a spring, to impact with the interior nose of the mole. The German Space Agency (DLR) developed a small mole for the Beagle 2 mission to Mars. In laboratory tests, this mole was capable of penetrating to a depth of 1.5 m in sand [4]. A similar, but larger device, the Mars Underground Mole (MUM) is currently being tested at NASA Ames Research Center [2]. As with other penetration methods discussed here, the low gravity environment presents issues pertaining to recoil and available reaction forces.

Ballistic Penetrometers: These are designed to impact the surface of a body at high speed and deploy a payload to the subsurface. Two previous Mars missions, Mars96 (failed on launch) and Deep Space 2 (failed at Mars) have attempted to use this technology. Currently, the Lunar-A mission, of the Japanese Space Agency, is planned to deploy two ballistic penetrometers that will impact the lunar surface at 285 m/s and deliver seismic and thermal instruments to a depth of 1-3 m [5]. All of these previous designs make use of

gravitational force to accelerate the penetrometer prior to impact. With a small asteroid or comet, the penetrometer would require a propulsion system to accelerate it.

References: [1] Richter, L., (2006) Personal Communication [2] Gonzalez, A. (2006) Personal Communication [3] Zacny, K., Glaser, D., (2006) Near Surface Rapid Soil Characterization System, DoD 2005.2 SBIR Phase I Proposal Topic A05-125 Proposal Number A052-125-3631 [4] Richter, L., et al. (2001) Adv. Space Research vol. 28, No. 8,pp. 1225-1230 [5] Mizutani, H., et al. (2005) http://www.ias.ac.in/jessci/dec2005/ilc-22.pdf

RADIOISOTOPE ELECTRIC PROPULSION AS AN ENABLER OF COMPREHENSIVE RECONNAISSANCE OF SMALL BODIES. Robert E. Gold, Ralph L. McNutt, Jr., Paul H. Ostdiek and Louise. M. Prockter, Johns Hopkins University Applied Physics Laboratory, 11100 Johns Hopkins Road, Laurel, MD 20723, U.S.A., Robert.Gold@jhuapl.edu.

Introduction: We are investigating a new class of missions that are well-suited to the study and characterization of small bodies. PARIS (Planetary Access with Radioisotope Ion-drive System) spacecraft take advantage of the high-efficiency of Stirling radioisotope generators (SRGs), currently in development, enabling low-thrust missions launched to a high C3. With a demonstrated efficiency of >30% and a specific power of > 8W/kg, the SRGs provide the power for an electric propulsion system, which is especially effective for exploring objects in a shallow gravity wells. The net power-to-mass ratio enables a reasonable science payload to be carried for a reasonable (e.g., New Frontiers-class mission) cost (Prockter et al., this meeting). A standard payload for such a mission could include wide-field and narrow-field cameras, a UV-Vis-IR spectrograph, gamma ray and neutron spectrometers, and plasma and energetic particle spectrometers, although payloads designed to investigate the interior of a target object, such as radar or lidar instruments, or seismic sensors, could be added. The power system would generate about 900 W and the launch mass would be slightly less than 1000 kg. Most technology for this class of missions already exists; the only technology development required is that of the next generation SRG, although this is currently in NASA's technology plan. With continued development, REP missions could be available for NEO characterization within the next decade.

PARIS Missions: The combination of radioisotope power sources (RPSs) with electric propulsion techniques and Evolved Expendable Launch Vehicles (EELVs) enables a new class of space missions to the outer solar system. These radioisotope-electric-propulsion (REP) missions appear to fit within the NASA New Frontiers class of medium-sized planetary missions. These low-thrust systems can operate for durations of several years to achieve very large velocity changes (Δ-V) of the order of 10 km s^{-1}. Oleson et al. [1] showed that trip times for planetary orbiter missions could be significantly reduced by: (1) using a medium class launch vehicle with an upper stage to provide initial velocities significantly greater than Earth escape, and (2) employing the REP system throughout the cruise phase to decelerate and shape the trajectory to arrive at the target with near zero relative velocity. Because they are low-thrust spacecraft, pure REP systems that do not have chemical thrusters to make rapid velocity changes, are best suited to orbital missions around bodies in small gravity wells. This propulsion approach is ideal for Near Earth Objects and other small bodies, such as the Jovian Trojans [2]. Several RPSs may be used to drive the electric thrusters, which may be either ion thrusters or Hall-effect thrusters. The optimum thruster choice is a balance between specific impulse and thrust level and so depends on the details of the particular mission. In our studies, power levels of about 1000 W lead to a good compromise among payload carrying capability, launch mass, and overall mission cost. Other studies [3, 4] have arrived at a similar conclusion.

Power Source: The key to REP missions is the power source, and the figure of merit for these sources is their power-to-mass ratio. The type of radioisotope thermoelectric generator (RTG) that was used to power the Galileo, Ulysses, and Cassini missions used decay heat from ^{238}Pu and thermoelectric converters to produce about 300 W from a 50 kg mass, equivalent to about 6 W/kg. These RTGs are no longer in production and a new, smaller power unit, the Multi-Mission-RTG (MMRTG), is identified for use on advanced Mars rovers. However, because of efficiencies of scale, the need to operate in a Mars atmosphere, and the addition of shielding, the MMRTGs will only produce about 2.4 to 3.0 W/kg. This would make them prohibitively massive for powering an REP mission to small bodies.

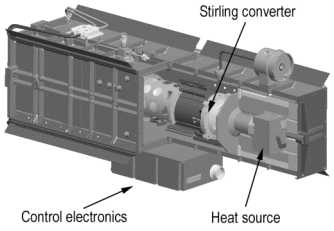

Fig. 1. First-generation Stirling power source.

Propulsion system: Ion and Hall-effect thrusters have been under development for many years. Electric thrusters have been used for station keeping of geosynchronous spacecraft, where low thrust is appropriate. The Deep Space 1 mission was the first application of electric thrusters to interplanetary missions. Current models of electric thrusters are sufficient to accomplish an outer solar system mission, and continuing development of these thrusters has greatly increased their longevity. Current ion engines are capable of surviving throughput of 120 kg of Xe

propellant, and improved designs and materials promise to extend that number by a large margin.

Spacecraft and mission design: Since REP missions are highly mass constrained, they require the use of the lightest components for each spacecraft function. A joint team of NASA Glenn Research Center and Johns Hopkins University Applied Physics Laboratory engineers and scientists has studied the spacecraft design. The team examined options ranging from how the spacecraft could be built today from existing components and materials to what improvements could be gained by the infusion of new technologies. They found that a practical spacecraft can be built with present-day components, but the development of several key technologies could significantly reduce the travel time and/or increase payload capacity. The spacecraft presented here is a design that can be built today using the classical RTG (approx. 5-6 W/kg), however, travel times can be dramatically improved with an improved high-density power source. The mission can be accomplished with any >4 W/kg power source with a penalty in travel time and available payload mass. The efficiency of the power distribution system is also key. A 20-cm or 30-cm ion thruster provides propulsion. Because of the anticipated long mission times and high Xe throughput, spare thrusters are included. The thrusters are mounted on a 2-axis gimbal to keep the thrust vector aligned with the center of mass. A conventional aluminum cylinder forms the core of the structure. To reduce the risk associated with a long mission, such as one that would visit 2 or more small bodies, the spacecraft design is fully redundant wherever possible. Fig. 2 shows a view of the PARIS spacecraft. The large communications antenna has electrically selected feeds so that it can communicate with Earth over all of the attitudes required for thrusting to a small body such as an NEO. The spacecraft dry mass is estimated to be 530 kg, including contingency, and the launch mass is 983 kg including 453 kg of xenon fuel. Launch would be on an Atlas V 551 with a Star 48 upper stage. Launch C_3 is 121.6 km^2/s^2. Electric propulsion Δ-V is 8.3 km s^{-1}. The nominal mission would orbit a small body for a year, to fully characterize it, then use its remaining fuel to visit and orbit a second small body to improve our understanding of the diversity of these objects.

Summary: REP systems offer cost-effective opportunities to study multiple small bodies within a single mission. Although REP missions are mass constrained, they can bring a comprehensive payload to explore NEO bodies, and have the potential to be a valuable tool in their characterization. REP missions are practical today, as long as the development of advanced RPSs continues.

References: [1] Oleson, S.R., et al., AIAA-2002-3967, Proceedings of the 38th Joint Propulsion Conference, Indianapolis, Indiana, July, 2002. [2] Gold R.E. et al., Proc. of the International Conference on Low Cost Planetary Missions, p.349-353. Kyoto, 2005. [3] Fiehler, D., and Oleson, S., *Acta Astronautica*, vol. 57, 444-454, 2005. [4] Bonfiglio, E. P., et al., AAS 05-396, Proceedings of the AAS/AIAA Astrodynamics Specialists Conference, Lake Tahoe, CA, 2005.

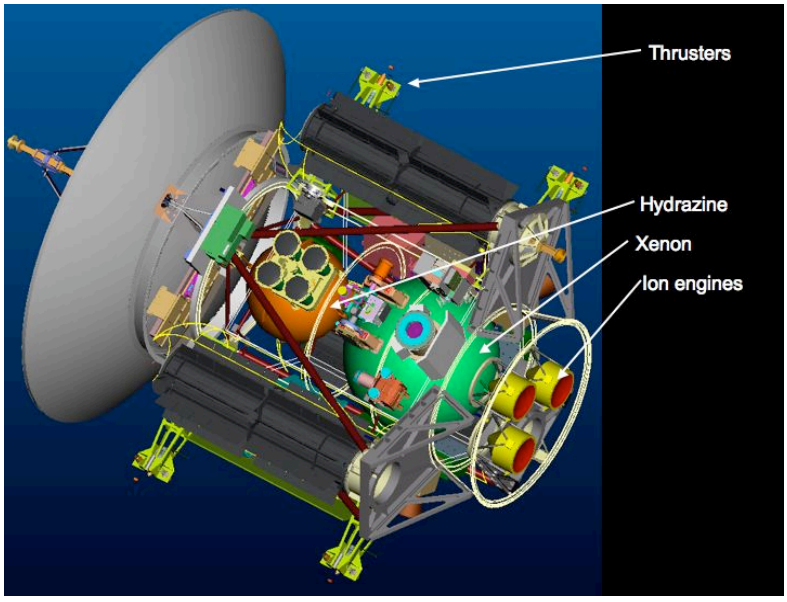

Figure 2. Partial cutaway drawing showing two of the Radioisotope Power Sources and the components of the ion propulsions system.

A STUDY OF TECHNIQUES FOR SEISMOLOGY OF ASTEROIDS. R. Goldstein[1], W. F. Huebner[1], J. D. Walker[1], and E. J. Sagebiel[1], [1]Southwest Research Institute, 6220 Culebra Road, San Antonio, TX 78238, rgoldstein@swri.edu, whuebner@swri.edu, jwalker@swri.edu, esagebiel@swri.edu

Introduction: Techniques to mitigate the potential threat to Earth of an approaching Near Earth Object (NEO) will require knowledge of the composition and structure of the body. In particular, information on the density, strength, and cohesiveness of the NEO will be necessary. Active seismology appears promising as a method of accomplishing such measurements. By "active" we mean a source (i.e. an impactor, thumper, or explosive) initiates a disturbance that propagates though the body and is detected by several sensors located on the body's surface. We have considerable experience in analyzing and modeling seismic signals in small bodies [1]; this study deals with methods of producing and recovering the seismic signals.

Versions of active seismology were used successfully on the moon during the Apollo 14, 16, and 17 missions. In fact, most of what we know about the interior of the moon was obtained in this manner. Note that although such other techniques as radio tomography from an orbiting or flyby spacecraft can also provide some aspects of internal structure this method is not useful for metallic objects.

Lander Packages: In the case of an NEO the difficulty of seismology lies in how to deliver and attach the sensors to such a low gravity body with a surface of a probably unknown nature. Providing a good acoustic contact between the surface and the sensor is a particular problem to solve. We have initiated a research program consisting of 1) Developing small lander packages and 2) Studying possible techniques for anchoring and providing good acoustic contact for these packages. We assume that the sensors and explosive signal source are launched to the body from an orbiting parent spacecraft, which also telemeters a source initiation signal and receives the seismic signals from the lander packages. Each package of our current baseline design consists of a commercial, off-the-shelf MEMS-based multi-axis seismometer together with a battery, associated electronics, and a telemetry system for sending the seismic signals to the orbiting parent. Since the MEMS-based sensors are very small and require very little power the package can be made small in size and low in mass. Thus several packages can be carried by the parent spacecraft. Figure 1 shows a diagram (taken from the Applied MEMS Inc. specification material) of the MEMS seismometer we plan to use.

Attachment/Coupling Studies: The difficulty in-designing a strategy for attaching the sensor packages and providing adequate acoustic coupling is exacerbated by the likelihood that the nature of the asteroid surface may be unknown unless preliminary observations by a "scout" spacecraft is possible.

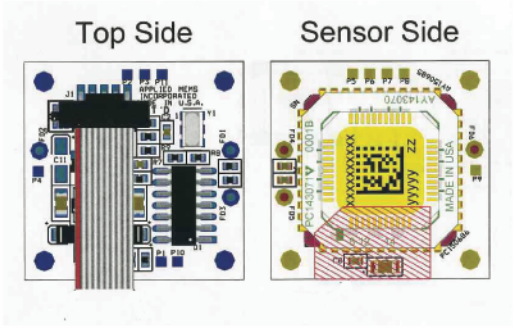

Figure 1. The circuit board of the MEMS sensor is 24.4 cm each side. The sensor itself is the yellow object on the right.

We assume the surface could range anywhere between a rubble pile with sandy deposits to a more cohesive structure. We have thus been considering use of two basic techniques for attaching the packages and providing adequate acoustic coupling: 1) impaling with a type of spike, and 2) coupling with an acoustically conductive adhesive or fluid. Our plans include testing these techniques in the Southwest Research Institute's seismic and gas gun facilities. Figure 1 shows a sketch of a concept for testing on a sandy or gravelly surface. To simulate the low gravity at an asteroid the test package is suspended from above to allow it barely to touch the surface.

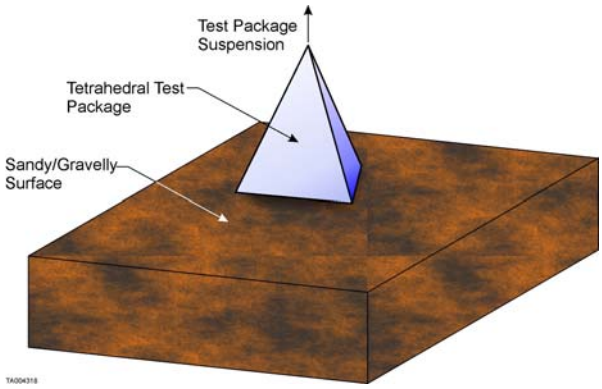

Figure 1. Schematic drawing (not to scale) of the proposed test setup for the case of the sensor package resting on the surface. The package will be suspended from above to simulate the very low gravity at an as-

teroid. The "bed" will be mounted on a seismic shake table to provide a controllable, known input signal.

A schematic block diagram of the electronics is shown in Figure 2. The low resource requirements of the MEMS seismometer allows a small, low power system.

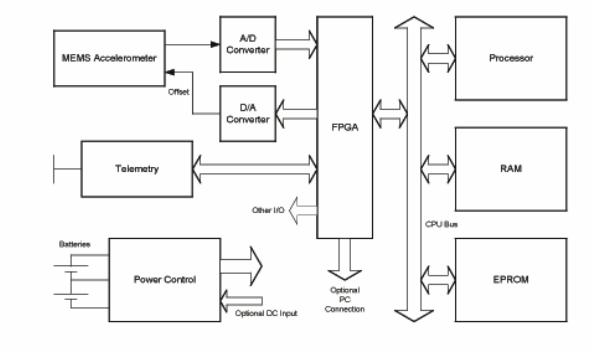

Figure 2. Example schematic block diagram of the sensor package electronics.

Summary: We have been studying techniques for performing seismology measurements on an asteroid in order to determine the body's internal structure. Such information is necessary in order to be able to mitigate the potential threat to Earth of an approaching NEO.

Reference: [1] Walker, J. D. et al., Global Seismology on Irregularly Shaped Bodies, 2006, this Conference.

Comet and Asteroid Sample Acquisition, Containerization, and Transfer for Sample Return

S. Gorevan, I. Yachbes, P. Bartlett, K.Zacny, G. L. Paulsen, T. Kennedy, B. Basso, J. Wilson
Honeybee Robotics, 460 West 34th Street, New York, NY 10001

Abstract

The authors have been instrumental in the development of three key sample return technologies. This was accomplished through their work at Honeybee Robotics supporting the Champollion-Deep Space 4 (figure 1) mission when that mission was baselined as sample return. Additionally they have provided support for the Mars Sample Return Mission 2001. Both missions were cancelled but not before an autonomous spacecraft rendezvous and docking interface, a hermetically sealable sample return canister, and a subsurface sample acquisition system were developed.

When NASA decided that the Champollion Deep Space 4 Mission would return surface and subsurface samples from a comet, Honeybee Robotics was contracted to supply the Sample Acquisition and Transfer Mechanism (SATM) (figure 2), a WEB (figure 3) docking interface, and a hermetically sealable sample return canister (SRC) (figure 4). The Champollion-DS4 mission in its sample

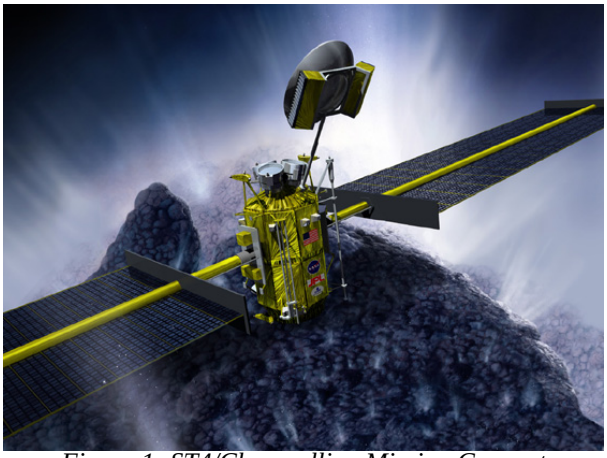

Figure 1: ST4/Champollion Mission Concept
Image courtesy of NASA/JPL

Figure 3: WEB docking system breadboard hardware. Lander (left) near capture with return spacecraft

Figure 4: Overhead view of 6 sample storage locations

Figure 2: Sample Acquisition and Transfer Mechanism drilling sequence

return configuration featured a surface lander that separated from a spacecraft that orbited the comet. The SATM robotically drilled down to 1 meter below the surface and acquired samples in the drill tip. The samples were transferred through mechanisms inside the SATM to the SRC. Dust mitigating seals developed by Honeybee allowed hermetic sealing to take place in a dusty environment. These seals were utilized by autonomously preloading the canister onto the comet surface to maintain the seal for the return cruise. After the samples were collected and the canister was sealed, a portion of the lander with the SRC lifted off from the comet surface to rendezvous and dock with the orbiting spacecraft. The SRC was mechanistically transferred to the orbiting spacecraft for the return cruise. The enabling feature of the WEB docking interface is the net like or spider web type capture element. This feature was unlike any known docking interface and like a spider, it provided for a wide field of capture. Using titanium barbs on the target spacecraft and a vectran web on the chase spacecraft, the target spacecraft was captured when any barb passed the web plane. The flexible web is then retracted pulling the target spacecraft toward each other down a misalignment correcting cone. The WEB docking interface compensated and corrected for extremely wide misalignments in x, y, z, pitch, and yaw and the web acted as a soft interface providing for significant dynamic misalignment as well.

The WEB docking interface is a cost reducing simple way to safely insure precision autonomous docking between two spacecraft. A sample return canister capable of preserving the sample during cruise and designed to be easy to transfer from the small body surface could be enabling to a sample return mission. The same is true for the SATM which not only can service a sample return mission but can also provide for the precision transfer of samples to instruments on board an in-situ characterization mission.

Cometary Materials Considered- Halley – Enke-B/Grigg-Skjellerup- Borrelly- Eros. I. E. Harris St Lambert, Quebec Canada.

Introduction: In order to appreciate the statistical concern with data from the comets noted in respect of Vega 1 data and Giotto data from comet Halley and others, it is necessary to envisage the missions. The best evidence is still the traverse of the probe through the ion trail and the dust trail at the point of such traverse -in the case of Halley with Vega at about 500 kilometres from the nucleus and in the case of B/Grigg -Skjellerup at a distance less that, a distance in which some differences were noted resulting in a postulation of mother molecules and daughter molecules. The mass spectrometer would confirm what the spectrograph had shown and there would be a counting of elemental atoms and molecules encountered in the tail to give confirmation of the spectrographic data already seen . However what we have is some operating stress on the nucleus and on the the tails involving magnetopauses and magnetic and other changes in the tails, at least, and neither instrument would pick up what could be a statistical problem relating to how the nucleus is being taken apart to create the dust and ion trails. As mentioned there is evidence of changes even within the tail itself at different distance from the nucleus. The reduced quantities of some common elements such as Fe in these statistics is an introduction to the problem of the statistical problem in relation to a sample from this examination point of the nucleus. [1]

Heavy elements are present :

Taken from the same work the elemental abundances of comet Halley were found as follows:

Element	Comet Halley	Sun
H	9.47	12.00
C	8.64	8.56
N	8.05	8.05
O	8.99	8.93
Na	6.58	6.33
Mg	7.58	7.58
Al	6.41	6.47
Si	7.85	7.55
S	7.44	7.21
K	4.88	5.12
Ca	6.38	6.36
Ti	5.18	4.99
Cr	5.53	5.67
Mn	5.28	5.39
Fe	7.30	7.51
Co	5.06	4.92
Ni	6.19	6.25

The elemental abundances in comet Halley, sun and solar system, normalized to Mg 9 log N(H) =12.00. However as a start, we have to look at what are the prevalent molecules considered as forming comets to see how the component is said to differ from normal CI or CAI material.

Molecule	Abundence	Method of observation
H 2 O	100	IR, products of disassociation (H, OH, O) in UV visible, and radio
CO	2-20	UV, radio
CO 2	3	IR
H 2 CO	0.03-4	Radio, IR
CH 2 OH	1-8	Radio, IR
HCOOH	Less than 0.2	Radio
CH 4	Less than 1	IR
NH 3	0.1- 1	Products of disassociation (NH, NH 2) in UV and visible
HCN	About 0.1	Radio
N 2	0.02-0.2	Products of ionization N 2 + in visible
H 2 S	About 0.2	Radio
CS 2	o.1	Products of disacciation (CS) in UV
OCS	Less than o.3	Radio, IV
SO 2	Less than 0.001	UV
S 2	0.05	UV

Abundances of mother molecules known in comets However this has to be compared with the spectrograph of various combinations detected in the comets to give a better idea of what is in fact present, as follows

Radical, ion or atom	Spectral domain
Radicals	
CN	Visible, IR
C 2	Visible, UV, near IR
C 3	Visible
CH	Visible
OH	Near UV, IR, radio
NH	Visible
NH 2	Visible
CS	UV
Molecular ions	
CH +	Visible
OH +	Visible
H2O +	Visible
CO +	Visible, UV
N 2 +	Visible
CO 2 +	Visible, UV
Atoms	
H	Visible, UV
C	UV
O	Visible, UV
S	UV
Na, K, Ca, Cr, Mn, Fe, Ni,Cu, Co, V	Visible comets near Sun
Atomic ions	
C+	UV
Ca+	Visible

As can be noted some of the heavier elements are noted as present under the atoms detected. There was upon review of these combinations and elemental problems of abundance issue raised, for instance, the isotope mesurement of carbon did not resemble that of interstellar medium, or of solar sytem and as the compostion ratios did not resemble those either which could be worked out given the material. Elsewhere in the study of the data in the Jacques Crovisier and Thérèse Encrenay it was said that from the isotope measurements there was a clear anology between cometary material and certain meteorites considered primitive - therefore considering the presence itself of some heavy elements as was noted in the data this would certainly entail an elemental list of abundances more like the Sun or CI .. There was other evidence moreover of the disparity with the data and what could be the nucleus in at least four other problematical considerations. The albeido of the nucleus was too low for the amount of water ice. And at .0.04 it could be only water ice coated with a crust or dark material presumeably carbon from the probe data.

The comet body was shown to be active in certain areas with gas and dust escaping, and this was difficult to explain in terms of the body of water ice..

Another factor was that the expected temperature of the sublimation of ice in a vacuum was 200 to 220 K or about -53 degrees C . The temperature detected at the surface of the nucleus was 300 degees K or about 27 degrees C - too high to explain sublimation of ice-indicating other process. Also this would be an overall temperature and perhaps not representative of the active areas, fully.

The rotation period of the comets is also a function of velocity and material make-up and the rotational period of the body at 16 to 18 hours at the velocity of 100,00 miles an hour might indicate a heavier more consistent body.

In summary there would seem to be a visible concern or biase in the data which would opt for a more solid nucleus of the comet with material coming off in particular process . Its importance is further on in the origin and reason for the occurrence of the comet ; and whether they come as one or in tandam as an example of the importance of the problem

[1] See Stuart Ross Taylor Solar System evolution - a new Perspective Cambridge University Press 1992 and 1994 at pg 1 23 where the Fe/Si and Mg/Si ratios are discussed -noted to be distinct from solar ratios and earth ratios and thought to come from dust component only of comet.

[2] Stuart Ross Taylor op.cit at pg 124, Table 3.10.2

[3] Jacques Crovisier, Thérèse Encrenay Les comètes- Témoins de la naissance du systéme solaire Belin CNRS edition Paris 1995 tables at pgs 48 and 103.

[4] Stuart Ross Taylor op cit in discussion of gas composition at pg 123 and cosmochemistry problems on same page and at pg 125 in discussioin of Fe/Si ratio and Mg/Si rations.

[5] Jacques Crovisier, Thérèse Encrenay op.cit a t pg 73.

DIELECTRIC PROPERTIES OF CHONDRITES AND THEIR IMPLICATION IN RADAR SOUNDING OF ASTEROID INTERIORS. E. Heggy[1], E. Asphaug[2], R. Carley[3], A. Safaeinili[4], and K. Righter[5]; [1]Lunar and Planetary Institute, Houston, TX, 77058-1113, USA (heggy@lpi.usra.edu); [2]University of California, Santa Cruz, CA, 95064, USA; [3]University of Cambridge, Cambridge, UK; [4]Jet Propulsion Laboratory, Pasadena, CA, 91109, USA; [5]NASA Johnson Space Center, Houston, TX, 77058-3696, USA.

Introduction: Over the past decades, radar remote sensing techniques have provided new insights into the surface and subsurface properties of the Earth, Moon, Venus, Mars, and Titan. Its demonstrated surface and subsurface imaging capabilities and mature spatialization techniques make it one of the most prominent techniques for exploring the interior of asteroids and providing a first insight into their geophysical properties, including volumetric images of the interior that assess their three-dimensional distribution of complex dielectric properties that reflect their structural, mechanical, and compositional variations. Such information is crucial for understanding the evolution of those objects as well as the potential hazard associated with any potential collision with other bodies of the solar system. The success of these radar investigations (as well as our understanding of the data acquired by earlier Earth-based radar observations) is strongly dependent on how the mineralogy, temperature, and porosity of the local environment affect the interaction of the radar wave with the surface and its propagation vector in the subsurface. Unfortunately, we have yet to characterize much of the potential parametric space associated with any of these planetary bodies. This research addresses this deficiency by determining the electromagnetic properties of a broad range of asteroid-like materials, mainly chondritic meteorite materials.

Experimental Approach: The radar penetration depth in geological materials for a given frequency can be constrained by quantifying the total signal loss affecting the radar wave during its propagation through the subsurface. Total signal loss can be summarized as the sum of individual losses from the surface reflection, geometrical spreading, electromagnetic attenuation, and scattering [1]. The amplitude of each loss mechanism is frequency and target dependent. At low frequencies (e.g., 1–50 MHz) the electromagnetic attenuation dominates the total signal losses and hence defines the penetration capabilities of a sounding experiment [2]. The electromagnetic properties in this study case is defined in term of the knowledge of the dielectric constant of the different units constituting the asteroid body and its evolution in term of the composition, density, and temperature variations among the structure. However, the parametric space associated with these dielectric properties has yet to be explored. In a first step toward addressing this deficiency we experimentally measured the electromagnetic properties of a broad range of dry meteoritic samples, mostly ordinary chondrites (LL5, L5, H5, and mesosiderites) inferred to have a good compositional analogy to asteroid material as observed from spectral observations [3,4]. Measurements were performed at room temperature using alternative current impedance techniques to evaluate the dielectric constant, represented by a complex variable ($\varepsilon^{/}$-i $\varepsilon^{//}$).

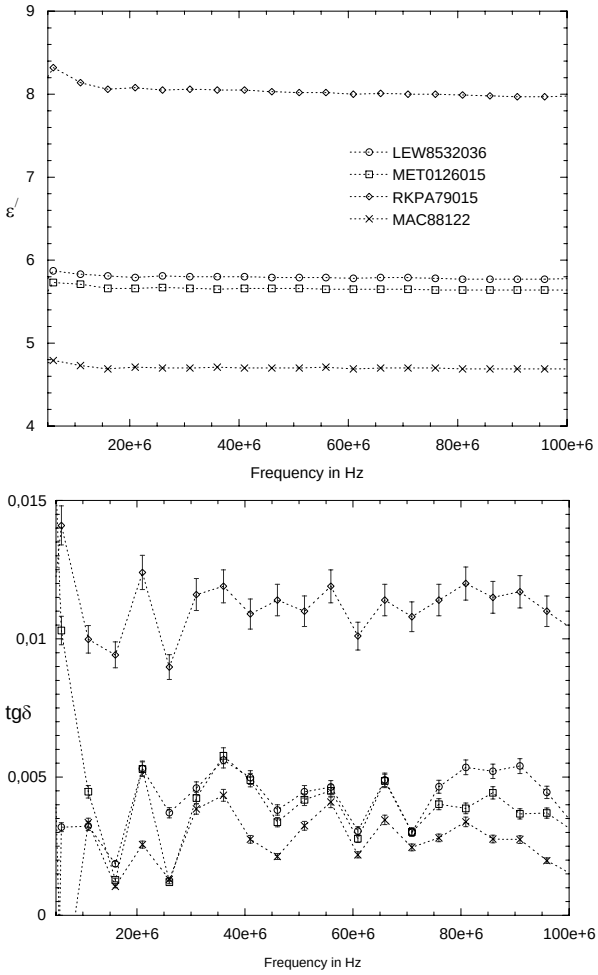

Fig. 1: Dielectric constant (upper) and the loss tangent (bottom) for dry chondritic samples in the frequency band 5–100 MHz at room temperature.

Measurements were made in the frequency range 1 MHz to 3 GHz with the dielectric cell connected to a high-precision impedance analyzer connected to a guarded coaxial capacitive cell designed to avoid field-

edge effects, which tend to reduce measurement accuracy. The use of guarded electrodes also prevents large reading errors in the lower limit of the frequency band where error exceeds 3%. Figure 1 summarizes some of the measurement results in the frequency band from 5 to 100 MHz for four chondrite samples: MAC 88122 (LL5), MET 0126015 (L5), LEW 8532036 (H5), and RKPA 79015 (mesosiderite) that are mineralogically and petrophysically characterized and curated in the Johnson Space Center meteorite database. We can clearly observe that the dielectric properties follow very closely the meteoritic classification with an increase of the dielectric constant as a function of the iron oxide enrichment of each meteorite class. The observed frequency dependence is very weak, suggesting a non-dispersive behavior for the chondrites. The real part of the dielectric constant is confined between ~4.6 and 5.8 for our samples with the exception of the mesosiderite, which contains a much higher amount of iron oxides than the other three samples and has a real value of ~8 at 20 MHz. While LL5, L5, and H5 samples can be viewed as representative of the outer layers of an asteroid [3], mesosiderites can be assumed as an analog to the denser metallic core material of an asteroid. The loss tangent values (bottom of Fig. 1), which are defined as the ratio between the imaginary and real part of the dielectric constant, are representative of the amount of signal losses in the radar wave [5] as they penetrate the asteroid outer layer to its central part. We can clearly note that chondrites have a very low loss tangent with an average value ~ 0.003 at 20 MHz for the LL5, L5, and H5 samples. This implies that such materials are very favorable to radar penetration.

In a first attempt to quantify this penetration depth using the laboratory experimental results, we calculated the theoretical two-way losses, α_{thl}, in dB/m and the associated theoretical penetration depth, δ_{thl}, in meters using a simple propagation model [equations (A) and (B), which do not consider scattering or magnetic losses] that integrates the dielectric constant and the loss tangent of the investigated materials as shown in Fig. 1. Hence for a given frequency, *f*, the radar losses and penetration depth are only a function of the permittivity as defined by equations (A) and (B):

$$\alpha_{thl} = 40 \times \frac{2\pi f}{c} \sqrt{\frac{\varepsilon'}{2}\left[\sqrt{1+(tg\delta)^2}-1\right]} \quad \text{(A)}; \quad \delta_{thl} = \frac{dB_{\max}}{\alpha_{thl}} \quad \text{(B)}$$

Figure 2 shows the evolution of the radar penetration as the function of the frequency for the average dielectric constant of 4.8 and loss tangent of 0.003 cited above for LL5, L5, and H5 samples as investigated in this preliminary study. The propagation model suggests that penetration depths of ~1000 m can be achieved at 20 MHz for an orbital sounder having a dynamic range of 60 dB.

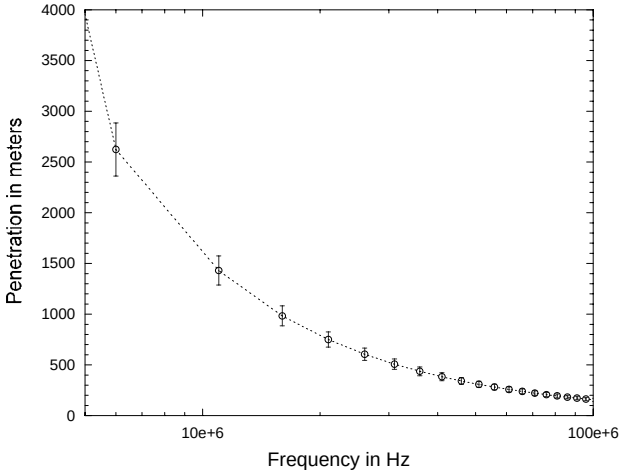

Fig 2: Penetration depth as a function of the frequency for an average asteroid represented by a typical chondritic sample.

It should be noted that the results in Fig. 1 are expected to vary significantly as the geophysical condition of temperature and density change the dielectric constant [6] and hence affect the penetration depth as can be deduced from equations (A) and (B). More parametric measurements are being performed by our team to quantify the effect of low temperatures and low density (inferred as a closer case to the asteroid environment) on the dielectric properties of asteroid analog materials (i.e., chondrites). Primary results suggest that both conditions cited above tend to decrease the dielectric constant and the loss tangent, which in turn improves the radar penetration depth capabilities.

References: [1] Reynolds (1997) *An Introduction to Applied and Environmental Geophysics*, Wiley, Chichester, England. [2] Heggy et al. (2006) *JGR-Planets, 111 (E6),* E06S04. [3] Binzel et al. (1996) *Bull. Amer. Astron. Soc., 28,* 1099. [4] Britt et al. (1996) *LPSC XXVI,* Abstracts, p. 167. [5] Ulaby et al. (1982) *Microwave Remote Sensing, Vol. II*. Artech House, Norwood, MA. [6] Heggy et al. (2001) *Icarus, 154(2),* 244–257.

Acknowledgments: This work is supported by the NASA Planetary Geology and Geophysics program through grant PGG04-000-0059 and the research fund of the Lunar and Planetary Institute.

DIELECTRIC PROPERTIES OF DIRTY-ICE AND FDTD SIMULATION OF RADAR PROPAGATION THROUGH COMET NUCLEI GEOELECTRICAL MODELS TO SUPPORT RADAR-PROBING INVESTIGATIONS OF COMET 67P/CHURYUMOV-GERASIMENKO. E. Heggy[1], R. Carley[2], W. Kofman[3], S. M. Clifford[1], A. Herique[3], I. P. Williams[4], and A. C. Levasseur-Regourd[5]; [1]Lunar and Planetary Institute, Houston, TX, 77058-1113, USA (heggy@lpi.usra.edu); [2]University of Cambridge, Cambridge, UK; [3]Laboratoire de Planétologie de Grenoble, Bât. D de Physique, B.P. 53, 38041 Grenoble Cedex 9, France; [4]Astronomy Unit, Queen Mary College, Mile End Road, London E1 4NS, UK; [5]Service d'Aeronomie, BP 3, 91371, Verrieres le Buisson, France.

The 90-MHz radar-wave experiment, CONSERT (COmet Nucleus Sounding Experiment by Radio wave Transmission), on board Rosetta (ESA, 2004) is expected to probe the nucleus of comet 67P/Churyumov-Gerasimenko (67P/C-G) to reveal information on its physical properties, composition, and internal structure through the radar inversion of the dielectric properties as deduced from the radar transmitted and backscattered echoes [1]. Hence the achievement of this task requires an adequate knowledge of the dielectric properties of such objects to constrain the ambiguities on future data inversion. As primitive building blocks of the solar system, an understanding of the composition and structure of comets will shed light on the conditions in the early planetary nebula at the time of planet formation.

The propagation of radar waves through the nucleus of comet 67P/C-G will be affected by the geometrical and petrophysical properties of the internal structure, as well as by its dielectrical properties determined by the nucleus porosity and composition. This investigation constrains the uncertainties of the dielectrical properties of comet-like materials inferred to be ice mixtures (dirty ice) and assesses the potentiality of recognition of structural elements in the comet nucleus with a radar experiment such as CONSERT. Geoelectrical models of sections of a comet nucleus, representative of existing theories of comet nuclei, will be presented to determine the effect of structural features such as layering and inclusions on the amplitude and losses of simulated transmitted and reflected radar waves as will be observed by CONSERT. Complex values of dielectric permittivity assigned to these models are based on laboratory dielectric measurements of a porous mixture of ice and dust as well as comparative values deduced from dielectric mixture law. We have used two types of dust in this study: meteoritic dust extracted from the grinding of different type of chondrites, and a typical basaltic dust extracted from the Craters of the Moon Volcanic Field in Idaho, USA.

Radar simulations at 90 MHz were carried out using the Finite Difference Time Domain (FDTD) method, which reproduce the transmitted and reflected electric field as a function of time. These results confirm that structural differences such as layers and inclusions are discernable from the comparison between transmitted and reflected radar signals.

Geoelectrical Models: In this investigation, the composition of comets is considered as a porous mixture of ice and dust, with values of complex permittivity measured and calculated for different porous mixtures of ice and dust. The principal ice in comets (~80%) is thought to be amorphous water ice [2] with minor constituents of carbon dioxide, carbon monoxide, and some organic species making up the remaining volatile content. Cometary dust, as observed in comet comae [3] and from Deep Impact [4], is a mixture of micrometer-sized grains of crystalline silicates such as pyroxene and olivine, with a composition range similar to that encountered in carbonaceous chondrites, along with smaller amounts of "light element" dust (carbon, hydrogen, oxygen, and nitrogen) in the form of complex or simple molecules. The dust content of comets may comprise up to 75% of the mass and 50% of the comet volume [5]. Non-gravitational effects on the motion and orbit of comet 67P/C-G have been used to place observational constraints on the density and porosity of the comet nucleus. The bulk density has been estimated with an upper limit of 600 kg m^{-3}, and the porosity as much as 70% [6].

Table 1 summarizes some of our dielectric measurements (real and imaginary parts in separate tables) at 90 MHz for ice mixtures with different type and mass concentration of dust inclusions at a temperature of –60°C and an average porosity of 55%.

	0%	25%	50%	75%
Basalt	2.67	3.62	3.84	4.03
LL5	2.67	3.21	3.44	3.72
H5	2.67	4.21	4.33	5.11
	0%	25%	50%	75%
Basalt	0.008	0.04	0.053	0.085
LL5	0.008	0.012	0.034	0.047
H5	0.008	0.056	0.066	0.091

Table 1: Measured dielectric properties of ice-dust mixtures (dirty-ice). Real part (upper) and imaginary part (bottom) at 90 MHz.

We considered in this preliminary study the dust to be basalt and chondrite inclusions into the pure ice.

For the chondrite dust we mainly considered typical chondrites from the LL5 and H5 classes. Different layers of the comet were simulated using different ice contaminated samples with different porosity levels ranging from 30% for the inner part to 70% to the outer part of the comet. Those parametric and frequency dependent measurements are then integrated in potential scenarios of the comet geoelectrical model that will serve as a support for the CONSERT data acquisition plan and analysis. Additionally, those geolectrical models are used as the entry parameter to the Finite Difference Time Domain (FDTD) simulations that help us understand the radar return from the sounding experiment.

FDTD Simulations: The FDTD algorithm uses the time-varying incident waveform to calculate the magnitude of the electric and magnetic fields within each "Yee cell" by solving Maxwell's equations. To simulate the electromagnetic wave emitted from the lander at the surface of the comet, a Gaussian pulse waveform, 15 ns long with a central frequency of 90 MHz, was applied to a model linear antenna aligned in the x direction in the center of the surface of the model geometry. The geoelectrical models were "meshed" into a three-dimensional grid of cubic "Yee" cells 0.25 m in size, each with specified electromagnetic properties. This dimension gives the calculation stability recommended value of ~10 cells per wavelength in the bulk of the material [7]. Reflections from the boundary of the simulation space were minimized by applying a Perfect Matching Layer (PML) algorithm that absorbs the electromagnetic fields at the boundaries of the simulation space with six layers of progressively decreasing permittivity. The magnitude of the total (scattered and incident) electric field in the two cross polarizations Ex and Ey were recorded at the top and bottom of the geoelectrical model to allow observation of the reflected and transmitted waveforms.

Results and Discussion: Simulation of the propagation of radar waves through different comet nuclei models has shown that it is possible for a radar experiment like CONSERT to distinguish structure in the comet nucleus by analysis of the amplitude and losses of the reflected and transmitted radar signals.

Although this study was only carried out for discrete sections of the comet model, it is clear that radar propagating through a body with different features such as layering and/or inclusions will present significantly different transmitted and reflected signals characteristics, allowing a non-ambiguous interpretation of the internal structure given an appropriate knowledge of the geoelectrical model of the comet. Of the models studied in this investigation, representing theoretical models of comet nuclei structure, the distinguishing features for each can be summarized:

Homogeneous nucleus: A reflected radar signal would only show reflections from a thick (>10 m) dust layer, and very small signals, particularly in the case of a very porous nucleus, from the other side of the comet due to the small dielectric contrast. The broadening of the waveform in transmission would also be related to the dielectric permittivity (determined by porosity and composition) of the comet nucleus. As reflections from a homogeneous nucleus are limited, the Ey component of the radar signal would be much smaller than the Ex component.

Layered nucleus: The presence of layers larger than the radar wavelength could be detected from reflected radar signals, but could be difficult to infer from the transmitted signal only. Thin, irregular layers representing heterogeneities within the comet nucleus would result in more reflection, scattering, and depolarization of the radar signal, similar to that produced by small inclusions.

Nucleus with inclusions: Inclusions in the comet nucleus cause reflections that result in a distorted waveform, and Ey component comparable in magnitude to the Ex component of the electric field. Inclusions significantly larger than the wavelength of propagation result in fewer reflections within the bulk of the nucleus, presenting a more homogeneous structure. This investigation has shown that large-amplitude transmitted and reflected signals could indicate the presence of many small inclusions, or fewer rocky inclusions, in the background icy matrix. This ambiguity could be resolved by constraints on the density and porosity.

The validity of the geoelectrical models presented in those simulations is based on the present-day knowledge of comet structure and composition. The *in situ* measurements carried out by the Rosetta lander will be able to offer improved estimates of the surface composition useful for radar data interpretation.

References: [1] Kofman et al. (1998) *Adv. Space Res., 21(11),* 1589–1598. [2] Rickman H. (1993) Cometary nuclei, in *Asteroids Comets Meteors* (A. Milani, ed.), Kluwer, Dordrecht. [3] Langevin Y. et al. (1987) *Astron. Astrophys., 187,* 761–766. [4] Harker D. E. et al. (2002) *Astrophys. J., 580,* 579–594. [5] Sykes M. V. and Walker R. G. (1992) *Icarus, 95,* 180–210. [6] Davidsson J. R. and Gutiérrez P. J. (2005) *Icarus, 176,* 453–477. [7] Yee K. S. (1966) *IEEE Trans. Antennas. Propag., 14(3),* 302–307.

POSSIBLE USE OF SURFACE CO_2 DETECTION VIA INFRARED SPECTROSCOPY TO INFER ASTEROID VOLATILE COMPOSITION. [1]C. A. Hibbitts, [1]Johns Hopkins University Applied Physics Laboratory, 11100 Johns Hopkins Rd., Laurel Md., 21045. karl.hibbitts@jhuapl.edu.

Introduction: Understanding the volatile content of asteroid surfaces could enable inference into interior compositions and structures. The presence of CO_2 in the surface of an asteroid would be evidence of a cometary component, its spectral characteristics would reflect the composition of the host material, and if its spatial distriubiton could be mapped, it would potentially provide insight into the presence of a remnant CO_2 reservoir.

Passive optical remote sensing is a powerful technique for surveying and characterizing asteroids. In particular, reflectance spectroscopy has provided insights into the general surface composition– basaltic, hydrous, anhydrous. The hydration state has been inferred through the presence of the ~3-micron water of hydration absorption feature [1,2]. The depth of the 3-micron band various within the C-class of asteroids, with the G subclass generally have a deeper band (> ~ 7%)) than the other subclasses (< ~ 3%), consistent with CM chondrites. Similarly, the larger M-class asteroids appear hydrated, while the smaller M-class have shallower or no 3-micron absorption bands [3], suggesting the larger hydrous M-class asteroids may be primitive. However, the less hydrated small M asteroids may simply have remained cold and ice could exist in their interiors [4]. Within the main belt, asteroids that are more affected by Jupiter (low Tisserand parameter) tend to be colored consistent with more primtive - redder and low albedo. Most asteroidal objects with T_j <3 have dark comet like albedos whereas only a few with T_j>3 do [5]. This suggests that asteroids affected by strong interactions with Jupiter tend to be more volatile rich than other asteroids. In fact, some extremely volatile-rich asteroids (main belt comets) can even possess tails and comas [6,7].

Discussion: Infrared measurements of CO_2 at ~ 4.25 μm in the surfaces would indicate the subsurface had (and may still have) a significant cometary component, even if not currently active. Observations of the Galilean satellites by NIMS show that CO_2 may be trapped into a surface, to exist stably for 'over geologic timescales' at temperatures well above the point where CO_2 ice would rapidly sublimate [8,9]. The spectral and spatial nature of the CO_2 on the Galilean icy satellites also imply that the CO_2 is endogenic, having outgassed from the interiors [10]. Furthermore, the largely-undifferentated interior of Callisto [11] continues to outgass CO_2, perhaps from a water-ice/CO_2 clathrate or solution [12] whereas the subsurface of Ganymed appears depleted [13].

The possibility that asteroids may contain a significant cometary componet suggests that CO_2 will be present on these more volative rich asteroids. CO_2 can remain physisorbed onto structurally complex clays for hours or longer when below 150K and has a spectral shape that depends on temperature as well as on the composition of the host material [14]. The spectral similarity between the nonice materials on the Galilean satellites (especially Callisto) and C-type asteroids [e.g. 15], suggests a compositional similariy. Thus, it is also possible asteroidal CO_2 would stably entrap into the asteroid surface so that if CO_2 exists or existed in the interiors of asteroids, some will also be observed in the surface.

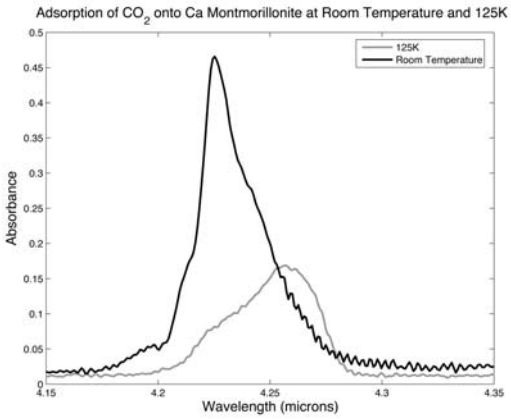

Transmission spectra of CO_2 physisorbed onto a thin sample pellet of powdered Ca-montmorillonite at room temperature (black line) and at 125K (gray line). The cold spectrum is similar to the shape of the feature on the Gallilean and Saturnain satellites. Stability at 125K to < 150K at ~ 1E-6 torr is > few hours.

References:

[1] Lebofsky et al, (1981) *Icarus*, 48, 453-459. [2] Rivkin et al., (2003) *Met. &Planet. Sci*., 38, 1383-1398. [3] Rivkin et al., (2000) *Icarus*, 145, 351-368. [4] Jones, et al., (1990) *Icarus*, 88, 172. [5] Fernandez et al., (2001) *ApJ*., 53, L197. [6] Hsieh et al., (2004) *Astron. J*., 127, 2997-3017. [7] Hsieh, J and D. Jewitt, (2006) *Science 312*, 561-563. [8] Carlson, (1996) *Science*, 274, 385-388; [9] McCord et al., (1998), *JGR*, 103, 8603-8626. [10] Hibbitts et al., (2000) *JGR*, 105, 22541-22557. [11] Anderson et al., (1998) *Science*, 280, 1573-1576. [12] Moore et al., (1999), *Icarus*, 140, 294-312. [13] Hibbitts et al., (2003), *JGR*, 108, 5036. [14] Hibbitts et al., (2006) *LPSC XXXVII*, abstract# 1753. [15] Calvin et al., (1991) *Icarus*, 89, 305-317.

WHAT ARE THE BULK PROPERTIES OF ASTEROIDS AND COMETS? Keith A. Holsapple, University of Washington 352400, Seattle, WA 98195. holsapple@aa.washington.

We now know a lot less about asteroids than we used to. Now we know they are not just big rocks: they come in many different forms and structure. We study their cratering and disruption, and design missions for science and for mitigation, but we know very little about the structural properties that determine these processes. And the success of any mission that actively interacts with their surface depends crucially on that structure.

One of the more fundamental classifications of these processes is the strength/gravity one. On Earth, cratering at small scales is strength dominated, but at large sizes it is gravity dominated. That transition occurs for craters of about 100 *m*, and scales as the inverse of the gravity for other bodies. For the catastrophic disruption of asteroids, the estimates for such a transition vary widely: from bodies with diameters as low as 100's of *meters* up to bodies with diameters of several 10's of *km*.

Deep Impact adds a new twist to this uncertainty. It has been widely reported that it was gravity dominated, based on observations of the ejecta plume. But I have concluded that there is no reason to suggest that the crater was gravity dominated. Furthermore, most of the outcome of Deep Impact is at odds with the conventional picture of cratering, including the ejecta velocities and the time scale of the plume. And the momentum imparted to Tempel 1 was from 20 to 200 times that of the impactor! It is more likely that the impact triggered the intrinsic energy of a comet outburst event.

This strength/gravity question is especially important regarding the protection of the Earth from the impacts of asteroids or comets. For small bodies a breakup is a distinct possibility. That threshold could be as low as the gravitational binding energy, which, for a 100 *m* object, is less than 10^2 *erg/g*! Or, if it is held together with strength, that energy could be several 10^6 *erg/gm*. In fact, the 370 *kg* Deep Impact impactor could break up a 600 *m* diameter object with mass density of 2 g/cm^3 if that object were only gravitationally bound! Could a simple science impactor such as envisioned for the ESA Don Quijote mission actually break up the target body? We don't really know.

And how do we land on and hold on to these bodies? Concepts such as space tugs, massive mass drivers, and the Bruce Willis concept of drilling into their surface to plant a nuclear bomb all require withstanding reaction forces and some method of attachment. Imagine putting your tent stakes into a dry sand surface even with 981 cm/s^2. Then take that gravity away and imagine the state of that sand! There is little point to driving a piton into such a surface.

I shall review what we know and do not know about the gross structure of asteroids and comets, and discuss the implications regarding a number of proposed science and mitigation missions. The planning and success of any mission must address those bulk properties of asteroids and comets.

This research was sponsored by NASA Grant NAG5-11446

Laboratory Simulations of Seismic Modification on Small Bodies. N. R. Izenberg[1], O. S. Barnouin-Jha[2] [1]noam.izenberg@jhuapl.edu, [1,2]The Johns Hopkins University Applied Physics Laboratory, 11100 Johns Hopkins Road, Laurel, MD

Introduction. Impact-induced seismic modification of small bodies in the solar system is probably a significant contributor to observed surface morphologies, and may be strongly affected by interior structure. To better understand how such a process actually operates on and in asteroids, we have constructed a seismic simulation mockup (SSM) and are conducting shaking experiments. Initial results indicate that seismic signals on a mostly competent body such as Eros can significantly alter surface morphology, generating downslope mass movements and modify or erase features in regolith.

Impacts on small bodies produce potentially substantial seismic signals [1-4]. Laboratory simulations of events on small bodies are providing insight on the connection between the competence or connectedness of asteroid interiors (shards vs. rubble-piles) and surface features (e.g. regolith development and modification, boulder distribution, "pond" development and crater degradation) [5,6]. Experiments like these could provide clues for better interpreting how asteroid interior structure influences observed surface morphology. Laboratory simulations may also inform development of active experiments for future asteroid exploration.

Seismic simulation mockup. The vibration lab at the Johns Hopkins University Applied Physics Laboratory (APL) is a spacecraft testing facility and a level 300,000 clean area. Reasonable precautions must be taken to keep particulate debris from the air and surfaces of the facility. The vibration tables (a T4000 shaker table) can be configured to induce both vertical and horizontal accelerations of up to a few gravities over amplitudes of a few centimeters. The SSM is essentially a 1 meter square, 40 cm deep Plexiglas sandbox, boltable to the table, designed to handle the accelerations of simulated seismic events. A Mylar lid prevents dust from escaping the experiments [7].

Initial experiments were conducted in open air conditions, using playground sand as a regolith simulant. We created angle of repose slopes and morphological features such as ridges and craters, and subjected them to simulated seismic signals including single jerks and sustained shaking of varying magnitudes and directions. Initial, intermediate, and final conditions were measured, and the experiments were recorded on analog video. Examples runs are shown in Figures 1 and 2.

Observations. The validation experiments have uncovered a number of empirical results we intend to quantify more rigorously with upcoming runs. Single jerks or seismic accelerations directing into a slope, in the upslope direction, do not induce much regolith movement on angle of repose slopes. Primary accelerations downslope or along slope both are much more effective at inducing downslope movements of material, as general creep downslope, larger landslides, or slumps of large amounts of slope material. Continuous oscillations of low acceleration do very little to modify slopes, but larger accelerations flatten regolith slopes rapidly and produce a hummocky "dynamic topography" that stays relatively unaltered even though the entire surface is moving relatively rapidly.

Larger pebbles move downslope at lower rates than smaller and lighter materials, and during rapid shaking, lighter, though not necessarily larger materials move constantly on the quaking surface. Crater forms, when subjected to single jerks exhibit landslide features primarily in the direction of the initial acceleration. Crater rims soften quickly, and only a few small or one large jerk can turn a crater in regolith into a dimple or make it disappear altogether.

Upcoming experiments include vertical shaking and mixed regolith (sand and larger materials) experiments. We will also be employing a high-speed camera to scale our experiments to lower gravity conditions.

References: [1] Richardson *et al.* (2004), *Science*, 306 1526-1529; [2] Thomas & Robinson (2005), *Nature, 436, 366-369;* [3] Greenberg *et al.* (1996), *Icarus,* 120, 106-118; [4] Horz & Schall (1981), *Icarus,* 46, 337-353; [5] Cheng *et al.* (2002), *Meteorit. Planet. Sci.* 37, 1095-1105; [6] Robinson *et al.* (2002), *Meteorit. Planet. Sci.* 37, 1651-1684. [7] Izenberg & Barnouin-Jha (2006) *LPSC* 37 #2017.

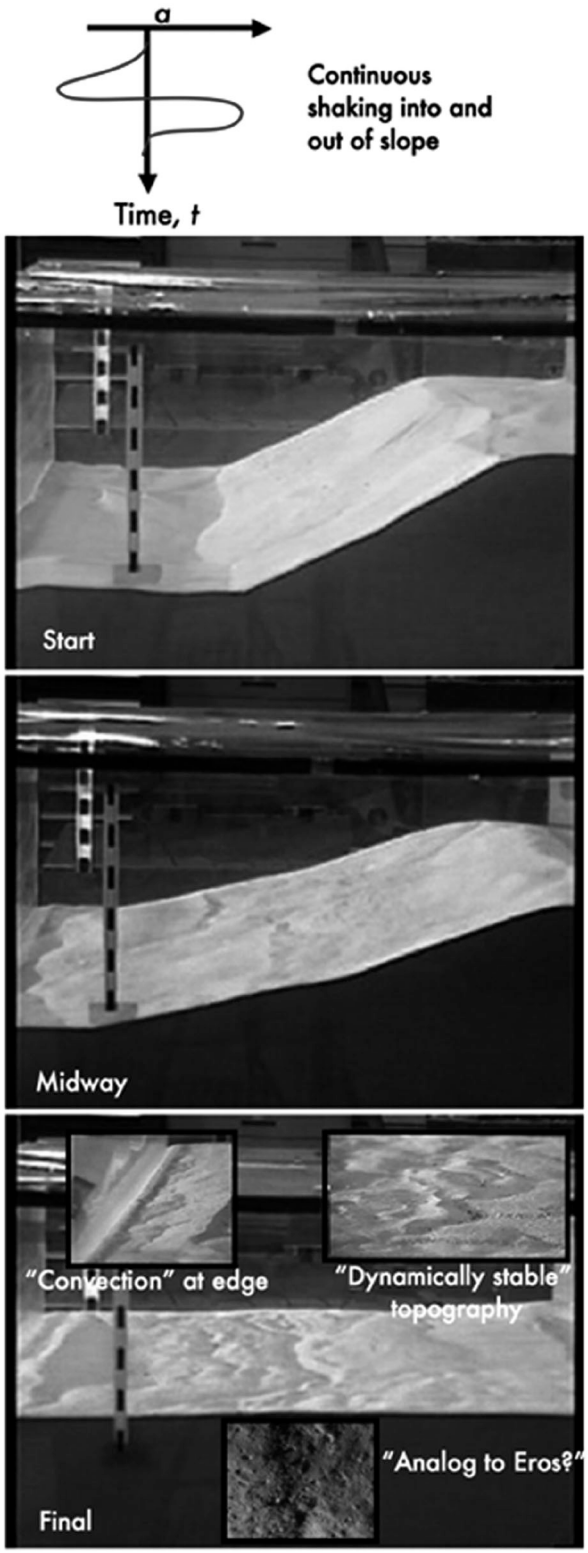

Fig. 1. Constant seismic shaking perpendicular to slope direction. Constant shaking of relatively small amplitude results in slope-flattening, convection of materials near barriers, and development of a "dynamically stable" surface topography.

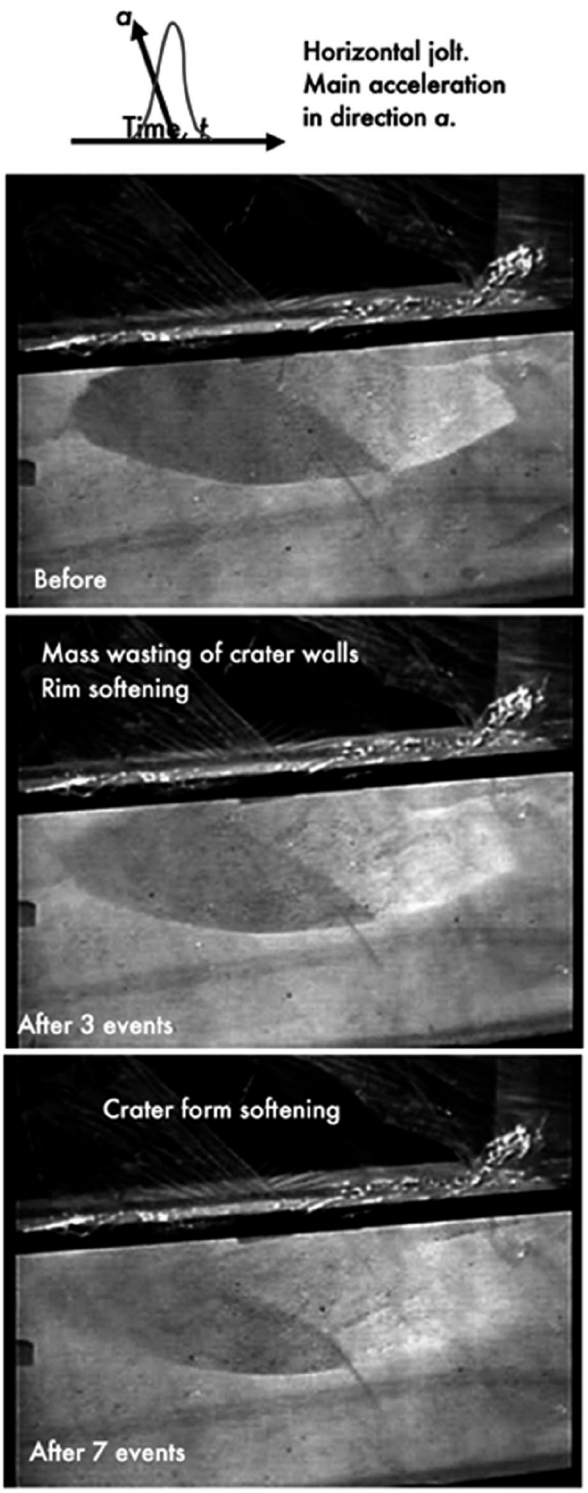

Fig. 2. Single seismic jerks of a crater form soften rim features and induce small slope failures and slides parallel to the direction of the primary seismic signals. Several jerks, (or a very few powerful jerks) "ghost" or remove the crater completely.

PROBING THE DEAD COMETS THAT CAUSE OUR METEOR SHOWERS. P. Jenniskens, SETI Institute (515 N. Whisman Road, Mountain View, CA 94043; pjenniskens@mail.arc.nasa.gov).

Introduction: In recent years, a number of minor planets have been identified that are the parent bodies of meteor showers on Earth. These are extinct or mostly-dormant comets. They make interesting targets for spacecraft reconnaissance, because they are impact hazards to our planet. These Near-Earth Objects have the low tensile strength of comets but, due to their low activity, they are safer to approach and study than volatile rich active Jupiter-family comets. More over, fly-by missions can be complimented by studies of elemental composition and morphology of the dust from meteor shower observations.

Meteor shower parent bodies: The first object of this kind was identified by Fred Whipple in 1983, when he realized that 3200 Phaeton moved among the Geminids [1]. The association was long disputed because the minor planet had the taxonomic type of an asteroid (type B) and the meteoroids had a relatively high density. Both aspects are now thought to be due to the low perihelion distance (q = 0.14 AU) of the orbit. At perihelion, they are heated to ~700 K, causing sintering of the dust grains into more solid particles.

The uncertainty was resolved in 2004, when a second such "asteroidal" looking minor planet 2003 EH1 was identified as the parent body of the Quadrantid shower [2]. The unusually steep inclination of the orbit (72^{o}) and its orientation made a chance association unlikely (chance of about 1 in 10^{5}). The stream is massive and about 500 years young, based on the dispersion of orbits. Given the lack of current activity of 2003 EH1, the stream was probably formed in a fragmentation event about 500 years ago. Chinese observers noticed a comet in A.D. 1490/91 (C/1490 Y1) that could have marked the moment that the stream was formed.

In 2005, a small minor planet 2003 WY25 was discovered to move in the orbit of comet D/1819 W1 (Blanpain). This formerly lost comet was only seen in 1819. A meteor outburst was observed in 1956, the meteoroids of which were traced back to a fragmentation event in or shortly before 1819 [3]. It was subsequently found that 2003 WY25 had been weakly active when it passed perihelion [4].

Since then, the Daytime Arietids have been found to be associated with the Marsden group of sungrazers [5], the alpha-Capricornids are associated with 2002 EX12, a weakly active comet at perihelion [5], and the Sextantids are from 2005 UD [6]. In all cases, the association has been established with reasonable certainty due to unusual orbital elements or the observation, or because of observed cometary activity from the proposed parent body. The list is increasing steadily. The observed meteor showers all have a relatively recent origin. The Andromedids date from 1843, the Phoenicds from 1819, the Quadrantids from 1490, the Daytime Arietids from a time after AD 1059. The Geminids date from around AD 1030. These dates define a historic event, the scars of which may still be recognized on the minor planet.

Type of fragmentation: Based on the number of showers of this type, this meteoroid stream formation mechanism is more important than water vapor drag of dust particles proposed by Whipple in 1950.

The most pressing issue is to discover the mechanism that is behind these fragmentation events. One clue from the meteor shower observations is the fact that the total mass of the meteoroid stream is often of the same magnitude as that of the remaining minor planet. That suggests that the fragmentation is due to the shedding of cometesimals, rather than catastrophic fragmentation.

The first direct evidence of this formation mechanism may have been detected during the 9P/Tempel 1 encounter of NASA's Deep Impact mission. Two regions on the comet surface were identified as the potential scars of such cometesimal shedding, each representing the loss of an ~0.5 km fragment [7]. It was later found that at these sites water ice is exposed near the surface [8]. The ice can be due to recondensation of a seep from a reservoir below the surface. The shedding of a cometesimal could have brought the reservoir to the surface, covering fresh ice by fallen back debris.

In this light, many of the surface features of other comets, such as 81P/Wild 2, are probably the result of cometesimal shedding.

References: [1] Whipple F.L. (1983) *IAUC* 3881, 1, 1983. [2] Jenniskens P. (2004) *AJ* 127, 3018. [3] Jenniskens P. and Lyytinen E. (2005) *AJ* 130, 1286. [4] Jewitt D. (2006) *AJ* 131, 2327. [5] Jenniskens P. (2006) *Meteor showers and their parent comets.* Cambridge University Press, Cambridge. [6] Ohtsuka K. (2005) Yamamoto Circular 2493, p. 2., November 14, 2005, S. Nakano ed., Oriental Astron. Assoc. [7] Jenniskens P. (2005) Meteor showers from broken comets. Abstract to conference Dust in Planetary Systems, Kaua'i, Hawai'i, Sept. 26-30, 2005. [8] A'Hearn M.F., *et al.* (2005) *Science* 310, 258.

Additional Information: More on this in: P. Jenniskens, 2006. *Meteor Showers and their Parent Comets.* Cambridge University Press (in press).

COLLISIONAL EVOLUTION OF COMETS

Z. M. Leinhardt and S. T. Stewart, Department of Earth and Planetary Sciences, Harvard University, 20 Oxford Street, Cambridge, MA 02138 (zoe@eps.harvard.edu, sstewart@eps.harvard.edu).

Introduction: To further our understanding of the initial conditions that produced our solar system we have begun to model the chemical and physical evolution of Oort Cloud comets and Kuiper Belt Objects (KBOs): the oldest, most volatile-rich, and most pristine objects in our solar system. Comets and KBOs are nearly as old as the Solar System and are the remnant building blocks of planets; thus they provide fundamental information about the initial conditions for the formation of planets. The parent bodies of KBOs were most likely formed in the outer regions of the Solar System while comets were most likely scattered into their current orbits by the giant planets. Neither comets nor KBOs have been perfectly preserved. Their surfaces have been weathered by high-energy particles, photons, and micrometeorites. Furthermore, impacts within the Kuiper Belt and between cometesimals (proto-comets) before scattering to the Oort Cloud are likely to have significantly altered the bulk chemical and physical properties from their initial state. We have begun conducting direct numerical simulations of collisions between cometesimals to investigate the evolution of the bulk properties of these objects. Our long-term goal is to determine the composition of the early protoplanetary nebula by modeling the evolution of cometesimals into present-day comets.

Numerical Method: The simulations are conducted using a shock physics code, **CTH** [1], which is coupled to an *N*-body gravity code, **pkdgrav** [2-4]. This method allows detailed modeling of the impact including heating, phase changes, and mixing of material as well as gravitational reaccumulation [Fig. 1].

CTH is a well tested Eulerian grid code that includes adaptive mesh refinement [Fig. 1a-b], which allows for the detailed modeling of impacts and cratering events. CTH also has the capability of modeling heating, multiple materials, mixed materials, and phase changes.

Once the initial shock wave and accompanying refractory wave have progressed through the target it is no longer necessary or practical to continue the simulation with CTH. At this point most of the shock induced physics is complete and gravity is the dominant force. Thus, the last output of CTH is run through a translator in order to convert the Eulerian grid data into Lagrangian particles, creating initial conditions for pkdgrav [Fig. 1c]. The gravitational evolution of the post-impact material is modeled under the constraints of self-gravity and physical collisions. The material of the original target and projectile are modeled as indestructible spheres that collide with one another inelastically. The particles cannot be fractured nor can they merge with one another.

Experiments: In previous work we tested our numerical method by conducting a series of catastrophic disruption simulations between single material asteroid-like bodies. These tests have confirmed that our hybridized numerical method produces results (mass of the largest post-collision remnant) consistent with other earlier numerical experiments [5-7]. Previous methods have not followed the gravitational reaccumulation; thus, in these cases the largest post-collision remnant is determined by ballistic equations. In our simulations the mass of the largest post-collision remnant is measured directly.

In this paper we will present results from three dimensional off-axis collision experiments between basalt and ice bodies. In these simulations we will follow the location and degree to which the reaccumulated material is shocked by the initial impact event. We will also determine the percentage of volatile loss do to the impact.

This study will determine the compositional distribution on the surface and interiors of the collision remnants, which may help explain the color diversity in the Kuiper Belt when surface weathering is taken into account. Future work will investigate the effect of various mixed internal configurations of ice, basalt, and micro- and macro-porosity on collision outcome with a primary goal to determine the level of devolatilization from collisional evolution. This future study will help to explain why none of the four comet nuclei that have been observed in detail (Tempel 1, Wild 2, Borrelly, and Halley) look similar either in surface features or shape.

Conclusions: New hybridized shock-*N*-body simulations will allow us to constrain the composition of the protoplanetary nebula of our own solar system. These simulations will show how small bodies in our solar system evolve and to help explain the diversity of objects in the Kuiper Belt.

References: [1] McGlaun, J.M., S.L. Thompson, and M.G. Elrick (1990) *Int. J. Impact Eng.* **10**, 351-360. [2] Stadel, .G. (2001), Ph.D. thesis, U.

Washington. [3] Richardson, D,C., et al. (2000) *Icarus* **143**, 45-59. [4] Leinhardt, Z.M., D.C. Richardson, and T. Quinn (2000) *Icarus* **146**(1), 133-151. [5] Benz, W. and E. Asphaug (1999) *Icarus* **142**, 5-20. [6] Melosh, H.J. and Ryan E.V. (1997) *Icarus* **129**, 562-564. [7] Leinhardt, Z.M. and Stewart S.T. (2006) *LPSC* **37**, 2414.

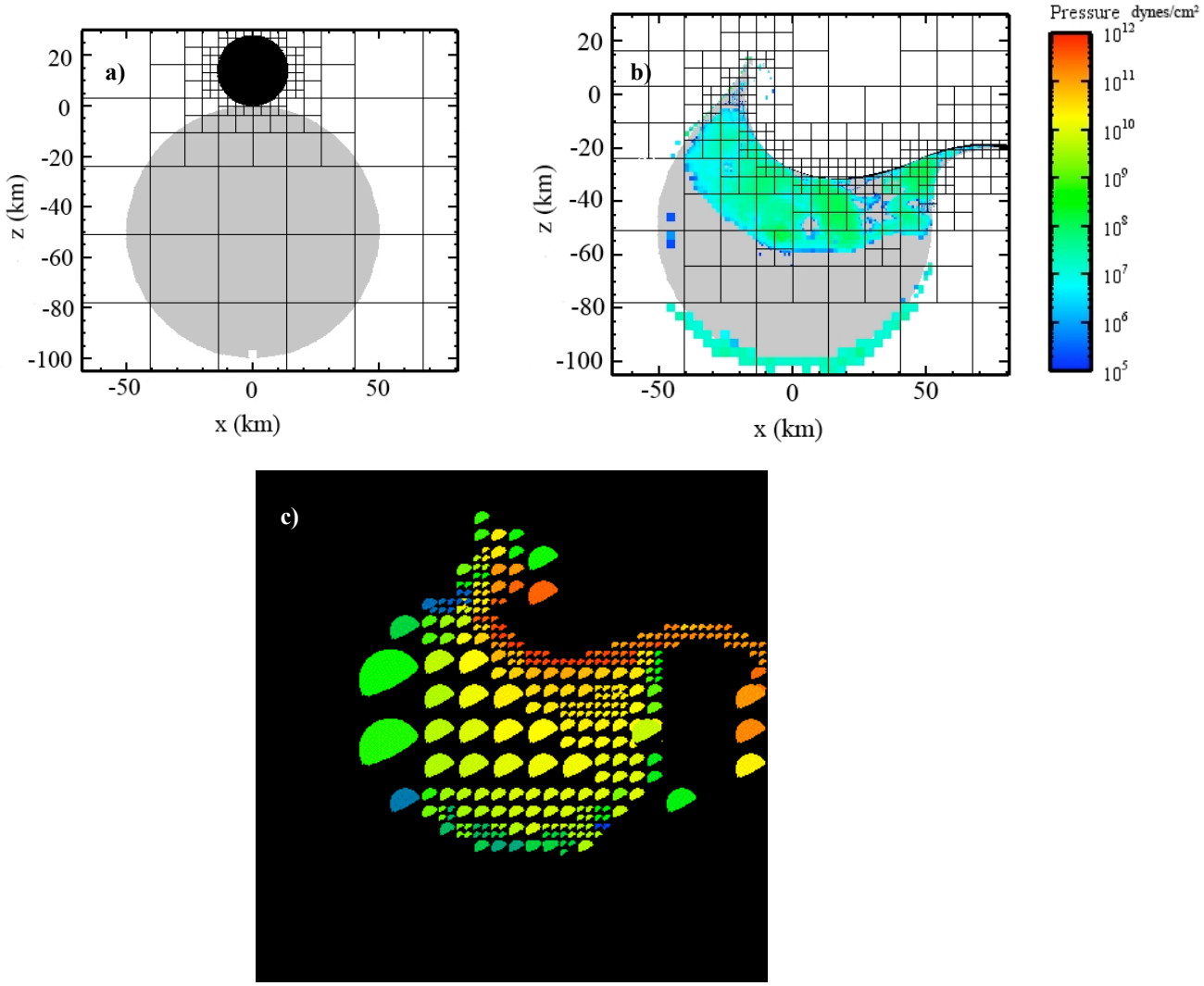

Fig. 1: An example of a hybridized impact simulation between two ice spheres. Frames a) and b) are modeled using the shock physics code CTH in 3-D, the plots are slices through the center of the impact along the y=0 plane. Frame c) is modeled using the 3-D *N*-body gravity code pkdgrav. Frame a) shows the initial condition in CTH. The grey sphere is a 50-km radius target, the black sphere is a 14-km radius projectile with an impact speed of 1.8 km/s. The grid overlayed on the frame represents the initial adaptive mesh refinement. Frame b) shows the result of the impact after 60 seconds. The hot color map shows the areas of highest pressure between 10^5 (blue) and 10^9 dynes/cm^2 (green). Frame c) shows frame b) converted into N-body particles and represents the transition from CTH to the gravity code pkdgrav. Frame c) is again a slice through the 3-D object along the y=0 plane. The colored particles represent grid blocks. These particles are color coded with respect to peak pressure attained over the first 60 seconds after impact (red = high pressure, blue = low pressure).